THE ASTROPHYSICAL JOURNAL, 506:495–501, 1998 October 20

COMPLEMENTARY MEASURES OF THE MASS DENSITY AND COSMOLOGICAL CONSTANT

MARTIN WHITE
Departments of Astronomy and Physics, University of Illinois at Urbana-Champaign, Urbana, IL 61801; white@physics.uiuc.edu
Received 1998 February 24; accepted 1998 June 1

ABSTRACT

The distance-redshift relation depends on the amount of matter of each type in the universe. Measurements at different redshifts constrain differing combinations of these matter densities and thus may be used in combination to constrain each separately. The combination of Ω_0 and Ω_Λ measured in supernovae at $z \lesssim 1$ is almost orthogonal to the combination probed by the location of features in the cosmic microwave background (CMB) anisotropy spectrum. We analyze the current combined data set in this framework, which shows that the regions preferred by the supernova and CMB measurements are compatible. We then quantify the favored region and also discuss models in which the matter density in the universe is augmented by a smooth component to give critical density. These models, by construction and in contrast, are not strongly constrained by the combination of the data sets.

Subject headings: cosmic microwave background — cosmology: theory

1. INTRODUCTION

There has recently been progress in observationally determining the cosmological redshift-distance relations, which in an FRW universe determine the contribution of various species to the total energy density. Two particular methods have advanced rapidly: the measurement of Type Ia supernovae (SNe Ia) as "standard" or "calibrated" candles at high redshift, and the angular size of features in the cosmic microwave background (CMB) temperature anisotropy power spectrum.

At low z the redshift-distance relation determines the deceleration parameter q_0, but as one goes to higher z the combination of densities that are constrained changes (see, e.g., Goobar & Perlmutter 1995). At extremely high z, as probed by the CMB anisotropies, the combination of densities that is probed can be nearly orthogonal to the combination given by q_0 (White & Scott 1996). Thus a combination of these two measurement techniques can isolate a small region in parameter space much more effectively than either of these methods independently.

There are two groups that have published data on the redshift-luminosity relation of SNe Ia at high z, and both groups appear to favor a low value of the mass density Ω_0 (see below). In addition, the current results on CMB anisotropies provide a lower limit on the angular scale of a peak in the spectrum. Such a lower limit provides an upper limit on the density of the universe in curvature, and thus a lower limit on Ω_0 in an open universe. In this paper we combine the current data on temperature anisotropies with the data on the SNe Ia redshift-distance relation. The purpose is threefold; the first and most important purpose is to point out that the contours of constant peak angular scale in the CMB and constant q_0 are nearly orthogonal in the observationally favored region of parameter space (see Fig. 1). The second purpose is to see whether the current measurements, taken at face value, are providing a consistent picture, and the third is to present the current status of the constraints and to indicate how we expect them to change in the near future.

Of course we expect rapid progress in both of these fields, and we are aware that a purely statistical analysis such as that presented here can miss the dominant sources of error; however, it seems timely to assess the level of agreement between these very different techniques for determining Ω_0 and Ω_Λ. The main conclusion of this work is that the two fields provide complementary information, which will of course bring robust changes to the data.

Finally, a word about notation: we assume the universe is described by an FRW metric with scale factor $a(t)$ and critical density $\rho_{\rm crit} = 3H_0^2/(8\pi G)$. Here $H_0 = 100\ h$ km s^{-1} Mpc^{-1} is the Hubble constant. We label the energy density, in units of $\rho_{\rm crit}$, from the various species as nonrelativistic matter Ω_0, cosmological constant Ω_Λ, and curvature Ω_K, where $K = -H_0^2(1 - \Omega_0 - \Omega_\Lambda)$. These densities must sum to unity: $\Omega_0 + \Omega_\Lambda + \Omega_K \equiv 1$. We define the dimensionless Hubble parameter $E(z)$ by

$$E^2(x = 1 + z) = \Omega_0 x^3 + \Omega_K x^2 + \Omega_\Lambda \, . \qquad (1)$$

In § 4 we will discuss the recently popular idea of a flat universe with a low matter density, the shortfall in energy density being made up in a "smooth" component that we call X. We shall see that in this model the combination of peak location and Ia distances is not as powerful a constraint.

2. REVIEW

Here we review some of the elementary material that will be used in this paper. This material is included for completeness and to define notation. The reader familiar with this is urged to skip to the next section.

2.1. *Luminosity Distance*

The SNe Ia results can be used to measure the luminosity distance back to a given redshift $d_L(z)$. The luminosity distance is related to the coordinate distance by

$$d_L(z) = \frac{1 + z}{\sqrt{|K|}} \sinh\,[\sqrt{|K|}\, r(z)] \qquad (2)$$

for $K < 0$. For $K > 0$, simply replace the sinh by a sin. At low redshift

$$H_0 r(z) = z\left[1 + (1 - q_0)\frac{z}{2}\right] \quad z \ll 1 \, , \qquad (3)$$

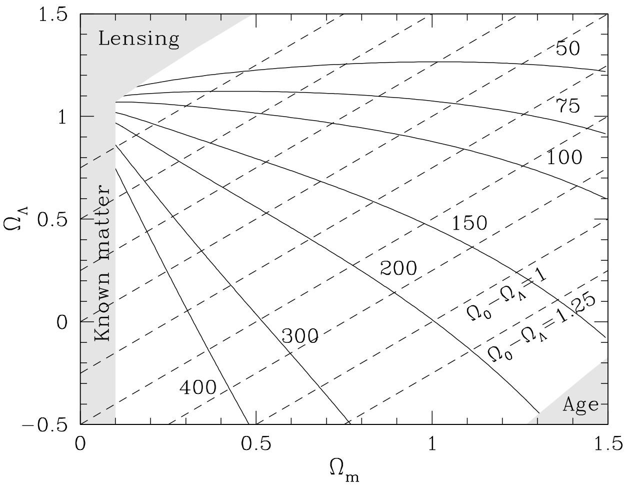

FIG. 1.—Contours of constant Ω_0-Ω_Λ (*dashed lines*, in steps of 0.25) and constant $\ell_{\rm peak}$ in models with adiabatic fluctuations in the Ω_0-Ω_Λ plane. We have taken $h = 0.65$ and $\Omega_b h^2 = 0.02$ for definiteness. There is a small [$\mathcal{O}(10\%)$] dependence of $\ell_{\rm peak}$ on these values as discussed in the text. Note that the contours are almost perpendicular in the observationally preferred region of parameter space. The shaded regions are ruled out by other constraints: $\Omega_0 < 0.1$ is inconsistent with the amount of matter observed, the lensing constraint is that the path length back to $z = 2$ cannot exceed 10 times the value in an Einstein–de Sitter universe, and for the age we have simply taken $H_0 t_0 > 0.6$ as a lower limit.

where $q_0 = (1/2)\Omega_0 - \Omega_\Lambda$. For the redshifts of relevance for the SNe Ia results, however, the low-z expression is not accurate. For arbitrary redshift

$$H_0 r(z) = \int_0^z \frac{dz'}{E(z')}\,, \tag{4}$$

which decreases to the present ($z = 0$).

Measurements of the redshift-luminosity relation are usually presented in terms of a distance modulus $m-M$ as a function of redshift. With the definition of absolute magnitude, M,

$$m - M = 5 \log_{10} \frac{d_L}{\rm Mpc} + 25 \tag{5}$$

$$m - M \simeq 5 \log_{10} \frac{cz}{H_0} + \cdots \; z \ll 1\,, \tag{6}$$

which is dependent on the value of h through the dependence in d_L. The measured magnitude, m, is independent of h, but the absolute magnitude, M, carries an h dependence that cancels that of d_L.

For $z \ll 1$ the distance modulus depends on Ω_0 and Ω_Λ only through the combination q_0; thus the slope of contours of constant $m-M$ in the Ω_0-Ω_Λ plane is $\frac{1}{2}$. As one goes to higher z, one must use equation (4), and the contours are no longer straight lines in this plane. However, since the curvature is "small" we can associate an approximate slope to these contours, which becomes steeper as z is increased. By $z = 0.4$ the slope is approximately 1 over the range of Ω_0 and Ω_Λ of interest. This increases to 1.2–1.3 by $z = 0.6$, 1.5–2 by $z = 0.8$, and 2–3 by $z = 1$. (The range indicates the curvature of the contours, which are steeper at higher Ω_0.) For the foreseeable future most of the SNe Ia will be at $z \sim \frac{1}{2}$, and therefore likely contours will be elongated along constant Ω_0-Ω_Λ.

2.2. *Angular Diameter Distance*

The presence of any feature in the CMB anisotropy spectrum with a known physical scale provides us with the ability to perform the classical angular diameter distance test at a redshift $z \simeq 10^3$ (see, e.g., Hu & White 1996a, Fig. 11). Perhaps the most obvious feature, and probably the first with angular size that will be measured, is the position of the first "peak" at degree scales in the angular power spectrum.

For any model in which no "new" component contributes at $z \simeq 10^3$, the positions of the peaks (features) in k space in the angular power spectrum depend only on the physical densities of matter $\omega_0 \equiv \Omega_0 h^2$ and baryons $\omega_b \equiv \Omega_b h^2$. We assume that the CMB temperature is well enough known to be "fixed," and that in addition to the CMB photons there are three massless neutrino species contributing to the radiation density at $z \simeq 10^3$.

The peaks arise because of acoustic oscillations in the photon-baryon fluid at last scattering, with photon pressure providing the restoring force, baryons the fluid inertia, and gravity the driving force (see, e.g., Bennett, Turner, & White 1997 for an elementary review). The assumption throughout this paper is that in adiabatic models the first peak represents a mode that is maximally overdense when the universe recombines. This peak is slightly broadened and shifted to larger angular scales by contributions from the Integrated Sachs-Wolfe effect (ISW; Sachs & Wolfe 1967) near last scattering (Hu & White 1996a).

In models in which the fluctuations are not purely adiabatic, causality requires that the features move to smaller angular scales, i.e., a higher multipole moment ℓ (Hu, Spergel, & White 1997). Thus in principle the measurements of a peak can provide only an *upper* limit on Ω_K. Measurements of the curvature independent of the model of structure-formation require information on smaller scale anisotropy (Hu & White 1996b, 1997). We shall henceforth assume that the fluctuations are adiabatic. This can be considered as adopting the upper limit on Ω_K as a measurement of Ω_K, which will be conservative for the purposes of this paper. Alternatively, one can argue that the adiabatic models are by far the best motivated and, in addition, are observationally preferred; therefore, we focus on their predictions. In the future, measurements of the whole anisotropy spectrum can allow us to relax this constraint. Under fairly reasonable assumptions (the fluctuations in the CMB are produced by gravitational instability, the baryon content is constrained by nucleosynthesis, secondary perturbations do not overwhelm the primary signal, etc.), these measurements can provide a model-independent measurement of the same combination of parameters as that constrained by $\ell_{\rm peak}$. As CMB measurements become more precise, we expect the "error ellipse" to be narrowed perpendicular to contours of constant $\ell_{\rm peak}$. (The length of the ellipse along the contour depends on signals other than the acoustic signature, which we will not consider here—it is this direction that is constrained by the SN.)

In order to proceed we have improved the approximation in Hu & Sugiyama (1995) and White & Scott (1996) by calibrating the position of the first peak in k-space by numerical integration of the Einstein, fluid, and Boltzmann equations. A fit that is accurate to better than 1% whenever

$0.1 \le \omega_0 \le 0.25$ and $0.01 \le \omega_b \le 0.025$ is

$$\frac{k_{\rm peak}}{\rm Mpc^{-1}} \simeq 0.0112 + 0.0441 w_0 - 0.043 w_0^2 - 0.0496 w_b + 0.162 w_0 w_b + 2.65 w_b^2 \ . \tag{7}$$

Any feature, e.g., $k_{\rm peak}$, then projects as an anisotropy onto an angular scale associated with multipole

$$\ell_{\rm peak} \equiv k_{\rm peak} r_\theta \ , \tag{8}$$

where r_θ is the (comoving) angular diameter distance to last scattering. In terms of the conformal time $d\eta = dt/a(t)$, we have

$$r_\theta = \frac{1}{\sqrt{|K|}} \sinh\,[\sqrt{|K|}(\eta_0 - \eta_*)] \tag{9}$$

for $K < 0$ negatively curved universes. For $K > 0$, merely replace the sinh with a sin. Note the similarity to the expression for $d_L(z)$ in equation (2). Here $\eta_*(\Omega_0 h^2, \Omega_b h^2)$ is the conformal time at last scattering. An accurate fit to the redshift of last scattering, $z_{\rm ls} \sim 10^3$, can be found in Appendix E of Hu & Sugiyama (1996). The conformal time at redshift z is given by

$$H_0 \eta(z) = \int_z^\infty \frac{dz}{E(z)} \ , \tag{10}$$

which increases to the present ($z = 0$). The accuracy of this projection for a range of models can be seen in Hu & White (1996b, Fig. 2), where it is seen to be good to $\mathcal{O}(15\%)$ except near the edges of parameter space. Slightly better agreement is obtained for the higher peaks or peak spacings, though we shall consider only the first peak here. In the figures we have corrected for the $\mathcal{O}(15\%)$ error induced by this approximation using the numerical computation of the anisotropy spectrum.

Note that since the anisotropy is being produced at $z \gg 1$, the contours have rotated to be almost orthogonal to those probed by the SNe Ia. The cosmological constant dominates only at late times, which make up most of the range of redshift probed by the SNe Ia. The conformal age today, however, probes most of the matter-dominated epoch and thus has a very different dependence on the density parameter and cosmological constant.

3. DATA

In this section we describe the statistical analysis of the existing data. We are of course aware that statistical uncertainties are not the only, and perhaps not the major, uncertainty in all of the data sets at this early stage. Of particular concern for SNe Ia are the effects of extinction in the host galaxy (but see Branch 1997) or differential reddening corrections between the distant and local/calibrating samples. For the CMB the difficulties associated with calibration and foreground extraction are the most worrisome. Here we shall describe our treatment of the statistical problem and leave the question of systematics to be determined by further data (see also Riess et al. 1998).

3.1. *Other Constraints*

Let us first begin by outlining the situation before the constraints from SNe Ia and the CMB are imposed (see also White & Scott 1996). The amount of matter in the universe inferred from dynamical measurements gives a lower bound on $\Omega_0 \gtrsim 0.1$, which rules out the region on the far left of our figures. The relative scarcity of gravitational lenses gives a *conservative* bound that the path length back to redshift $z \sim 2$ be $\lesssim 10$ times the Einstein–de Sitter value. This rules out the upper left-hand corner, which anyway would be ruled out by requiring the presence of a big bang or by the existence of high-z objects (Caroll, Press, & Turner 1992). We have imposed a constraint on the lower right-hand corner of the figure that the age of the universe $H_0 t_0 > 0.6$, which corresponds to 12 Gyr for $h = 0.5$. This is less conservative than the other limits, but that region is not observationally preferred.

A model-dependent upper limit to $\Omega_0 + \Omega_\Lambda$ comes from the *COBE* data that constrain $\Omega_0 + \Omega_\Lambda \lesssim 1.5$ under reasonable assumptions about the initial power spectrum of fluctuations (White & Scott 1996). We have not shown this region as shaded because of the model dependence of the constraint. Further discussion of constraints can be found in White & Scott (1996).

3.2. *Supernovae*

Two teams have been finding high-z SNe Ia suitable for measuring the $d_L(z)$ relation. The Supernova Cosmology Project (SNCP) has published data on eight SNe, of which six can be corrected for the width-luminosity relation (Perlmutter et al. 1997, 1998).[1] The High-z Supernova Search has published data on 10 SNe (Garnovich et al. 1997; Riess et al. 1998).[2] In addition, a set of low-z "calibrating" SNe has been obtained by the Calan-Tololo group (Hamuy et al. 1996). We use the 26 SNe with $B-V < 0.2$ described in Hamuy et al. (1996).

For simplicity we use only the B-band observations for all of the SNe. For the Hamuy et al. (1996) sample, the observational errors on $\log_{10}(cz)$ were added in quadrature to the quoted errors on the (uncorrected) peak magnitude using the fact that at low z the slope of the magnitude $\log_{10}(cz)$ relation is 5. We performed a maximum likelihood fit to the combined data set as follows. First, for a given point $(\Omega_0, \Omega_\Lambda)$ we computed the expected function $m_B(z)$ with a given absolute brightness M_B of SNe Ia. Each of the data points was then width-luminosity–corrected using a linear relation (Hamuy et al. 1996)

$$m_{{\rm corr},B} = m_B - \alpha(\Delta m_{15} - 1.1) \ , \tag{11}$$

where Δm_{15} is the number of magnitudes the SNe Ia declines in the first 15 days (Phillips 1993; in several of the Calan-Tololo SNe Ia the light curves do not start until 10 days after the peak; therefore in this case Δm_{15} is obtained from a fit to a template SNe Ia in the B, V, and I bands). For fixed α the errors on Δm_{15} and m_B were added in quadrature, which ignores a potential for correlated errors from photometric uncertainties affecting the light-curve fit. These correlations are not quoted by any of the groups, although they are included in the fit by the SNCP team (S. Perlmutter 1998, private communication). Including such correlations

[1] For more information regarding the Supernova Cosmology Project, see the High-Redshift Supernova Search Home Page at http://www-supernova.lbl.gov/.

[2] For more information on the High-z Supernova Search, see http://cfa-www.harvard.edu/cfa/oir/Research/ supernova/HighZ.html.

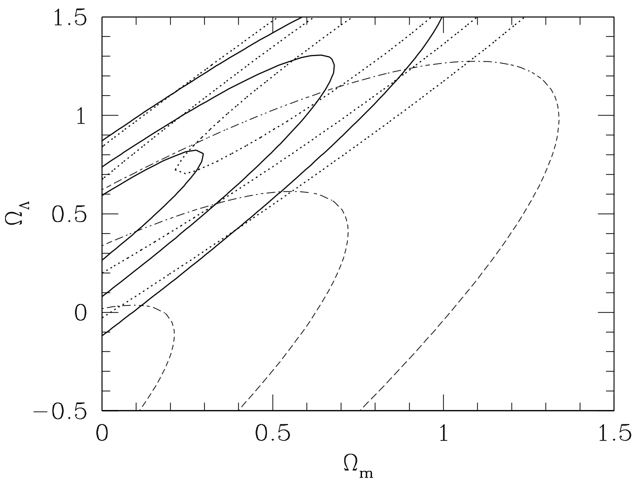

FIG. 2.—Likelihood in the Ω_0-Ω_Λ plane for fitting the SNe Ia data described in the text. The dashed lines are 1, 2, and 3 σ contours for fitting the low-z results plus the SNCP data. The dotted lines are for fitting the low z plus the High-z Supernova Search data, and the solid lines are for fitting all of the data.

would only serve to tighten the allowed regions; therefore, it is conservative to neglect them. Performing an χ^2 fit of the data to the theory then allows us to calculate

$$\mathscr{L}(\Omega_0, \Omega_\Lambda, M_B, \alpha) = \exp\left(-\frac{\chi^2}{2}\right). \tag{12}$$

This likelihood is then marginalized over M_B with a uniform prior and over $\alpha = 0.784 \pm 0.182$ (Hamuy et al. 1996), where the error is assumed to be Gaussian. The result is $\mathscr{L}(\Omega_0, \Omega_\Lambda)$, which is shown in Figure 2.

Note that this method is not exactly equivalent to the analysis performed by either of the groups whose SNe data we have used. In particular, we have used only a subset of the data (the B band), we have used equation (11) rather than a multicolor light-curve shape method, and we have marginalized over the absolute brightness of SNe Ia and slope of the width-luminosity relation in equation (11). By marginalizing over α and M_B the fit is allowed to find the best value for the combined data set rather than fixing, e.g., M_B from the low-z sample alone. We find that the maximum likelihood point (Ω_0, Ω_Λ, M_B, α) is a reasonable fit to the data, being allowed at a 96% confidence level (CL). The subset excluding the High-z Supernova Search data fares better: it is allowed at a 78% CL. The subset excluding the SNCP data is allowed at a 93% CL. The best fit to all of the data has M_B less than 1 σ from the best fit to the Hamuy et al. (1996) data, although before marginalization the data prefers a higher value of $\alpha \simeq 1.1$. Again excluding the High-z Supernova Search data, the best fit prefers $\alpha \simeq 0.784$ in agreement with Hamuy et al. (1996). Given all this, the results of the marginalization procedure should be very close to the alternative method of maximizing $\mathscr{L}(\Omega_0, \Omega_\Lambda)$ over α, M_B. Indeed, the contours derived here will likely compare well with those in Perlmutter et al. (1998) and Riess et al. (1998).

3.3. *Anisotropy*

The observational situation with regard to anisotropy measurements on degree scales, which can pin down the location of the first peak in the spectrum, is not as advanced as that for the SNe. It is common procedure to constrain cosmological models (usually variants of cold dark matter, or CDM) by fitting theories to a collection of "bandpowers." For current data this provides a good approximation of the results of a full likelihood analysis (Bond, Jaffe, & Knox 1998). Recent work using this method gives $\ell_{\rm peak} \sim 260$ (Lineweaver 1998) or $\ell_{\rm peak} = 263^{+139}_{-94}$ (Hancock et al. 1998; the error is almost symmetric in log ℓ). This would constrain Ω_0 in an open universe to $\Omega_0 \gtrsim 0.4$ (95% CL; Lineweaver 1998; Hancock et al. 1998).

Some of the weight against low-Ω_0 models in the above fits comes from the fact that low-Ω_0 CDM models typically predict a "dip" in power before the rise into the first peak. This dip comes about because the ISW effect provides an increase in large-angle power while both the ISW effect and the acoustic oscillations in the baryon-photon fluid provide a rapid rise in power into the first peak. This leads to a "dip" in power just before the rise into the first peak that is constrained by the present data. However, since the behavior on angular scales larger than the peak can be model-dependent, we must be careful in applying the limits quoted above.

Perhaps the most conservative estimate of the location comes from the analysis of Hancock et al. (1998), who in addition to CDM models fit a phenomenological model first proposed by Scott, Silk, & White (1995). This phenomenological model does not contain the dip and thus penalizes the high-$\ell_{\rm peak}$ models based only on the information around the peak. It is on the basis of this model that they quote a marginalized peak position $\ell_{\rm peak} = 263^{+139}_{-94}$, which we have used in Figure 3.

3.4. *Combined Constraint*

The allowed regions from the SNe Ia, CMB peak, and constraints discussed in § 3.1 are shown in Figure 3. Since the current CMB data do not unambiguously show a well-defined peak, we have been cautious in plotting the allowed CMB region. The contours shown cover the region $\ell_{\rm peak} \lesssim$

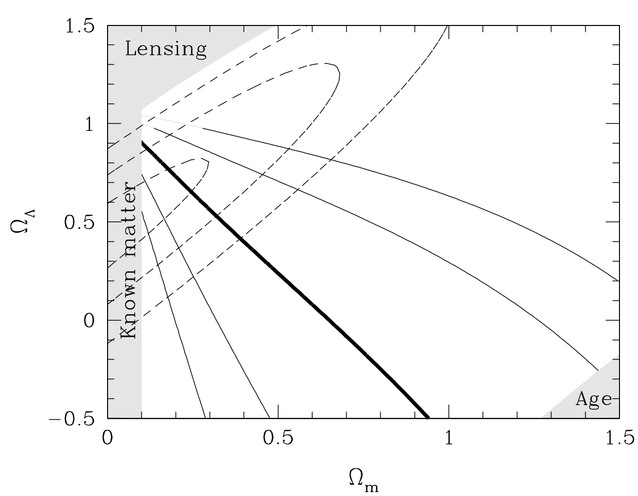

FIG. 3.—Likelihood in the Ω_0-Ω_Λ plane for fitting both the SNe Ia and CMB data described in the text. The dashed lines are 1, 2, and 3 σ contours for fitting the SNe Ia results, and the solid lines are the CMB results. The heavy solid contour represents the peak of the likelihood found by Hancock et al. (1997), and the two contours to either side represent conservative ± 1 and 2 σ values. The shaded areas are the same as in Fig. 1.

550 (*lower left*) to $\ell_{\rm peak} \gtrsim 130$ (*upper right*). This corresponds approximately to a 95% CL. The 2 σ limit at low ℓ is stronger than twice the 1 σ error quoted above since the likelihood function is non-Gaussian (Hancock et al. 1998). The upper limit at $\ell \simeq 550$ is probably less firm than the lower limit, for which there is more data, and is quite sensitive to the results of the Cambridge Anisotropy Telescope CAT experiment (Scott et al. 1996). For a given (e.g., CDM) model it is possible to obtain stronger constraints on the parameters Ω_0 and Ω_Λ, but even the model-independent constraint is quite promising.

4. SMOOTH COMPONENT

The discussion until now has been focused on the "traditional" cosmological parameters Ω_0 and Ω_Λ; however, it has recently become fashionable to postulate the existence of a heretofore unknown component whose contribution to the energy density makes $\Omega_{\rm tot} = 1$, or equivalently $\Omega_K = 0$. Here we shall refer to this component as X, indicating its unknown nature. For the purposes of this paper all we need to know about X CDM is that it is smooth on scales smaller than the horizon and that its equation of state is $w \equiv p_X/\rho_X$, which we shall further assume is a constant. We will require that $w < 0$ so that X-matter is only contributing appreciably to the energy density at low z. X-matter will serve here as an example of a different set of distance redshift relations that can be probed by the combination of SNe Ia and CMB anisotropy measurements.

Various examples of X CDM and references are given in Turner & White (1997). A particularly appealing example of X-matter is a scalar field, which has been treated in detail recently by Coble, Dodelson, & Frieman (1997) and Caldwell, Dave, & Steinhardt (1998) (see also Ferreira & Joyce 1997), although the idea goes back much further (see, e.g., Kodama & Sasaki 1984). In this case there is the probability that w will vary with time, which will modify the results presented below as discussed later.

We also comment briefly on more exotic possibilities. When adding a new component the behavior of the background spacetime and the perturbations are governed by the stress-energy tensor of the new component(s). In Turner & White (1997) the new component was agnostically approximated as perfectly smooth, i.e., the perturbations in the stress-energy tensor were neglected. For a scalar field this is quite a good approximation well below the horizon, though it has been noted (Caldwell et al. 1998) that such a prescription is gauge-dependent and thus unphysical on scales larger than the horizon. If one assumes that X-matter is a scalar field in addition to the smooth component, one needs only to specify one fluctuating component: the energy density (which is related to the pressure and velocity fluctuations). All other fluctuations are zero. This can be generalized by allowing for a nonvanishing anisotropic stress (or "viscosity") that leads to "generalized" dark matter (Hu 1998), which has many nice properties. This model is called generalized because specifying the density, velocity, pressure, and anisotropic stress of the new component completely specifies the scalar part of the stress-energy tensor. Of course, beyond generalized dark matter one can include not only scalar (density) perturbations but vector and tensor perturbations and multifield models. All of these possible additions will have observable effects on the CMB anisotropy spectrum and large-scale structure. The parameter space is so large, however, that we shall concentrate simply on X-matter with constant w. Under this assumption, $\rho_X \sim a^{-3(1+w)}$. Two familiar limits are $w = -1$ for Ω_Λ and $w = -\frac{1}{3}$ for Ω_K.

Assuming that the vector and tensor components, anisotropic stress, and two-field isocurvature component are negligible, the only effect of X-matter on the CMB primary anisotropy spectrum is to change r_θ (eq. [9]) and modify the large-angle anisotropies. We can calculate $\ell_{\rm peak}$ merely by generalizing $E^2(x = 1 + z)$ to include a component $\Omega_X x^{3(1+w)}$ in the calculation of r_θ. The redshift-luminosity distance is only affected by the background energy density contributed by X-matter, which again is completely encoded by $E(z)$.

The situation with respect to large-angle anisotropies (e.g., as probed by *COBE*) is more complex. The simplistic assumption that X-matter be completely smooth cannot be exact on length scales approaching the horizon. A calculable example is provided by scalar field models. As discussed by Caldwell et al. (1998), although a scalar field is *approximately* smooth the deviations from this can affect large-angle anisotropies, and hence the *COBE* normalization (Bennett et al. 1996; Hinshaw et al. 1996; Gorski et al. 1996; Banday et al. 1997; we have used the method of Bunn & White 1997 to normalize these models). Indeed, by comparing the results of Turner & White (1997) with a calculation of the scalar field case with constant w we find that the fluctuations can give up to a 30% correction to the large-scale normalization in the range $0.2 < \Omega_0 \leq 1$ and $-1 \leq w < -\frac{1}{3}$ with the trend being worse agreement for higher w and lower Ω_0. For $w \lesssim -\frac{2}{3}$ or $\Omega_0 \gtrsim 0.4$, the correction is negligible (the data currently prefer $w \approx -1$). Unlike the case of precisely smooth X-matter, the scalar field matter power spectra are not very well approximated by the often used Γ-models once $w \neq -1$ (Bardeen et al. 1986; Hu 1998, Fig. 4). The sense is to reduce the ratio of small- to large-scale power as w is increased (i.e., made less negative) with the decrease occurring around the sound horizon at scalar field domination. For $w \lesssim -\frac{2}{3}$ and $\Omega_0 \gtrsim 0.3$, the correction is $\lesssim$20%, but for larger w can be a factor of 5. This makes the extrapolation to small scales more model dependent.

Unfortunately, if we believe that X-matter is a scalar field, the motivation for assuming a constant w is somewhat weak. While we can define an "average" value of w to use for calculating $\ell_{\rm peak}$, the effect on the large-angle anisotropies is more complex. The situation for generalized dark matter, cosmic strings, and textures is even more uncertain. Here anisotropic stress can play a large role, as pointed out by Hu (1998), and can lead to potentially large modifications of the large-angle anisotropies. Thus for these models the *COBE* normalization should be treated as highly uncertain—though the trend is to decrease the normalization over the $w = -1$ case. For general X-matter the best normalization currently comes from the local abundance of rich clusters (see Wang & Steinhardt 1998 for a discussion); however, without an independent normalization to which to compare it, this cannot be considered as a strong constraint on the model.

For these reasons we will focus on smaller angular scales, where the anisotropies were generated before X-matter became dynamically important. Specifically, we will focus on $\ell_{\rm peak}$ and treat w as an appropriate average value occurring in $E(z)$. If we ignore the large-angle ISW effect (which can be obscured by cosmic variance) and the effects of gravitational lensing on the small-scale anisotropy, then models that hold η_0, and the physical matter and baryon densities fixed, will result in degenerate spectra. For our purposes this means they will predict the same $\ell_{\rm peak}$ no matter how we choose to measure it. Hence X-matter introduces only one extra parameter (not time varying function) to be constrained by $\ell_{\rm peak}$. Unfortunately, while $\ell_{\rm peak}$ is insensitive to the details of X-matter, and because we have kept the spatial hypersurfaces flat, it also does not show the large variations seen in the Ω_0-Ω_Λ plane. Given the embryonic state of the CMB peak measurements to date, the peak location provides little constraint. Thus X-matter serves as an example, where the combination of CMB and SNe Ia results does not highly constrain the parameter space (as yet) in contrast to the standard Ω_0-Ω_Λ case.

We show in Figure 4 the 1, 2, and 3 σ contours in the Ω_X-w plane from the full SNe Ia data set. This updates Figure 4 of Turner & White (1997). Contours of $\ell_{\rm peak}$ are superposed on Figure 4 to show that the predicted location of the peak is quite insensitive to changes in Ω_X. These contours are for $h = 0.65$ and $\Omega_b\, h^2 = 0.02$, and changing these parameters can affect $\ell_{\rm peak}$ by $\mathcal{O}(10\%)$. The approximation discussed in § 2.2 is only expected to work to $\mathcal{O}(15\%)$, which is about the amount by which $\ell_{\rm peak}$ changes in the X-matter case. Thus we have used a full numerical computation of $\ell_{\rm peak}$ in making this figure.

The region near $\Omega_0 = 0.3$ is allowed for $w \approx -1$, in agreement with earlier studies (Coble et al. 1997; Turner & White 1997; Caldwell et al. 1998). Additional constraints such as the shape of the matter power spectrum as measured by galaxy clustering, high-z object abundances, and the abundance of rich clusters today do not alter this conclusion. While enhanced SNe Ia measurements will pick out a strip in the Ω_0-w plane, strong constraints on X-matter scenarios will probably have to await the upcoming satellite CMB anisotropy missions, especially if w changes at high z. Even with CMB satellites, accurate CMB measurements will have difficulty in determining Ω_X and $w_{\rm eff}$ precisely and simultaneously unless they can probe high-enough ℓ to see the effects of gravitational lensing. [Lensing depends on the matter power spectrum, which probes a different combination of parameters than $\eta_0(\Omega_X, w) = $ const, breaking the $\Omega - w$ degeneracy that enhances the marginalized errors.] Thus the combination of CMB and SNe Ia results will be important even in the *Microwave Anisotropy Probe* (*MAP*) era.[3]

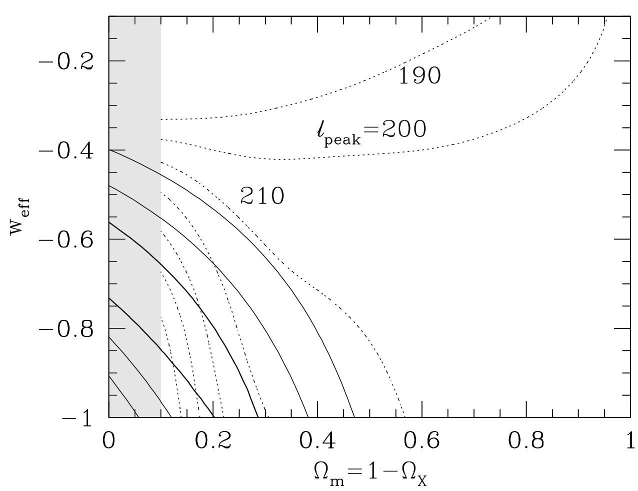

FIG. 4.—Likelihood in the Ω_0-w plane for fitting the SNe Ia data described in the text. Solid lines are 1, 2, and 3 σ contours. The dotted lines represent contours of constant $\ell_{\rm peak}$ for $h = 0.65$ and $\Omega_b\, h^2 = 0.02$ in steps of $\Delta\ell = 10$.

5. CONCLUSIONS AND THE FUTURE

We have examined the constraints in the Ω_0-Ω_Λ plane arising from a combination of SNe Ia and CMB data. Our most important result is that the two data sets provide approximately orthogonal constraints and therefore nearly maximal complementarity. We have illustrated this by a likelihood analysis of the current data. Even though very different uncertainties affect the two data sets, the likelihood functions are compatible with the allowed region shown in Figure 3. As more data are acquired, the combination will serve as an important cross check.

Because of current fashionability and for contrast we have also looked at constraints on universes with flat spatial hypersurfaces and low Ω_0, with $1 - \Omega_0$ in a smooth component called X. As expected, the constraints on this model are much weaker since—by design—the CMB peak location varies little with the model parameters. The allowed region is near $w \approx -1$ and the CMB peak does not prefer any value of Ω_0 within this region.

What about the future of this enterprise? Both the SNCP and the High-z team have ~ 50 SNe still to be analyzed, which should shrink the contours in Figure 2 considerably. Multicolor data will help control the uncertainty due to reddening, and the allowed region should lie along a line of slope $\simeq 1$ (most SNe Ia will be at $z \sim 1/2$) in the Ω_0-Ω_Λ plane with width ± 0.1. On the CMB front, data from currently operational experiments could determine the location of the peak in ℓ to $\Delta\ell \lesssim 30$ within the next year (assuming the peak is near $\ell \simeq 250$). From Figure 1 we see that such a measurement of $\ell_{\rm peak}$ would be comparable, but orthogonal, to the SN constraint. The first such experiment, the Mobile Anisotropy Telescope, has already had a "season" in Chile.[4] The Viper telescope[5] is operating at the South Pole, and results from several other experiments (see Bennett et al. 1997; Table 1) are expected this year or next. And of course we anticipate that *MAP*, scheduled for launch in late 2000, will determine $\ell_{\rm peak}$ to a few percent, with the precise number depending on the angular scale of the peak.

I would like to thank Joanne Cohn for a careful reading of the manuscript, Wayne Hu for useful conversations on generalized dark matter and scalar fields, Bob Kirshner and Saul Perlmutter for discussions on the SN constraints, Douglas Scott for comments on the manuscript, and Limin Wang for communication before publication about his work on the cluster abundance.

[3] For more information regarding the *MAP* era, please see http://map.gsfc.nasa.gov/.

[4] For more information on the Mobile Anisotropy Telescope see http://dept.physics.upenn.edu/~ www/astro-cosmo/ devlin/project.html.

[5] For more information regarding the Viper telescope see http://cmbr.phys.cmu.edu/vip.html.

REFERENCES

Banday, A., et al. 1997, ApJ, 475, 393
Bardeen, J. M., Bond, J. R., Kaiser, N., & Szalay, A. S. 1986, ApJ, 304, 15
Bennett, C. L., et al. 1996, ApJ, 464, L1
Bennett, C. L., Turner, M. S., & White, M. 1997, Phys. Today, 1997, 50, 11
Bond, J. R., Jaffe, A., & Knox, L. 1998, preprint (astro-ph/9708203)
Branch, D. 1997, MNRAS, 290, 360
Bunn, E. F., & White, M. 1997, ApJ, 480, 6
Caldwell, R. R., Dave, R., & Steinhardt, P. J. 1998, Phys. Rev. Lett., 80, 1582
Carroll, S. M., Press, W. H., & Turner, E. L. 1992, ARA&A, 30, 499
Coble, K., Dodelson, S., & Frieman, J. 1997, Phys. Rev., D55, 1851
Ferreira, P. G., & Joyce, M. 1997, Phys. Rev. Lett., 79, 4740
Garnavich, P. M., et al. 1997, preprint (astro-ph/9710123)
Goobar, A., & Perlmutter, S. 1995, ApJ, 450, 14
Gorski, K., et al. 1996, ApJ, 464, L11
Hamuy, M., et al. 1996, AJ, 112, 2398
Hancock, S., Rocha, G., Lasenby, A., & Gutierrez, C. M. 1998, MNRAS, in press
Hinshaw, G., et al. 1996, ApJ, 464, L17
Hu, W. 1998, ApJ, in press
Hu, W., Spergel, D. N., & White, M. 1997, Phys. Rev., D55, 3288
Hu, W., & Sugiyama, N. 1995, ApJ, 444, 489
———. 1996, ApJ, 471, 542
Hu, W., & White, M. 1996a, ApJ, 471, 30
———. 1996b, Phys. Rev. Lett., 77, 1687
———. 1997, ApJ, 479, 568
Kodama, H., & Sasaki, M. 1984, Prog. Theor. Phys., 78, 1
Lineweaver, C. H. 1998, in IAU Symp. 183, Cosmological Parameters and the Evolution of the Universe (Dordrecht: Kluwer), in press
Perlmutter, S., et al. 1997, ApJ, 483, 565
———. 1998, Nature, 391, 51
Phillips, M. M. 1993, ApJ, 413, L105
Riess, A., et al. 1998, preprint (astro-ph/9805201)
Sachs, R. K., & Wolfe, A. M. 1967, ApJ, 147, 73
Scott, D., Silk, J., & White, M. 1995, Science, 268, 829
Scott, P. F. S., et al. 1996, ApJ, 461, L1
Turner, M. S., & White, M. 1997, Phys. Rev., D56, 4439
Wang, L., & Steinhardt, P. 1998, preprint (astro-ph/9804015)
White, M., & Scott, D. 1996, ApJ, 459, 415